Journal of Physics: Conference Series **455** (2013) 012009 doi:10.1088/1742-6596/455/1/012009

Light-flavour identified charged-hadron production in pp and Pb–Pb collisions at the LHC

Roberto Preghenella for the ALICE Collaboration

Centro Studi e Ricerche e Museo Storico della Fisica "Enrico Fermi", Rome, Italy
Sezione INFN, Bologna, Italy

E-mail: preghenella@bo.infn.it

Abstract.

Thanks to the unique detector design adopted to fulfill tracking and particle-identification (PID) requirements (e.g. low momentum cut-off and low material budget), the ALICE experiment provides significant information about hadron production both in pp and Pb–Pb collisions. In particular, the p_{T}-differential and integrated production yields of identified particles play a key role in the study of the collective and thermal properties of the matter formed in high-energy heavy-ion collisions. Furthermore, the production of high-p_{T} particles provides insights into the property of the hot medium created in such collisions and the in-medium energy-loss mechanisms.

Transverse momentum spectra of $\pi^{\pm}$, $\mathrm{K}^{\pm}$, p and $\bar{\mathrm{p}}$ are measured at mid-rapidity ($|y| < 0.5$) over a wide momentum range, from $\sim$ 100 MeV/c up to $\sim$ 20 GeV/c. The measurements are performed exploiting the $\mathrm{d}E/\mathrm{d}x$ in silicon and gas, the time-of-flight and the ring-imaging Cherenkov particle-identification techniques, which will be briefly reviewed in this report. The current results on light-flavour charged-hadron production will be presented for pp collisions at $\sqrt{s} = 0.9$, 2.76 and 7 TeV and for Pb–Pb collisions at $\sqrt{s_{\mathrm{NN}}} = 2.76$ TeV. Integrated production yields, transverse momentum spectra and particle ratios in pp are discussed as a function of the collision energy and compared to previous experiments and commonly-used Monte Carlo models. Pb–Pb collisions at the LHC feature the highest radial flow ever observed and an unexpectedly low p/π production ratio. The results are presented as a function of collision centrality and compared to RHIC data in Au–Au collisions at $\sqrt{s_{\mathrm{NN}}} = 200$ GeV and predictions from thermal and hydrodynamic models. The nuclear modification factor (R_{AA}) of identified hadrons will also be discussed and compared to unidentified charged particles and theoretical predictions. This is observed to be identical for all particle species at high-p_{T}.

1. Introduction

ALICE (A Large Ion Collider Experiment) is a general-purpose heavy-ion detector at the CERN LHC (Large Hadron Collider). It has been designed in order to fulfill the requirements to track and identify particles from very low ($\sim$100 MeV/c) up to quite high ($\sim$100 GeV/c) transverse momenta in an environment with large charged-particle multiplicities as in the case of central lead-lead (Pb–Pb) collisions at the LHC.

The ALICE experiment, shown in Figure 1, consists of a central-barrel detector and several forward detector systems. The central system covers the mid-rapidity region ($|\eta| \leq 0.9$) over the full azimuthal angle. It is installed inside a large solenoidal magnet providing a moderate magnetic field of 0.5 T. It includes a six-layer high-resolution inner-tracking system (ITS), a large-volume time-projection chamber (TPC) and electron and charged-hadron


Content from this work may be used under the terms of the Creative Commons Attribution 3.0 licence. Any further distribution of this work must maintain attribution to the author(s) and the title of the work, journal citation and DOI.
Published under licence by IOP Publishing Ltd

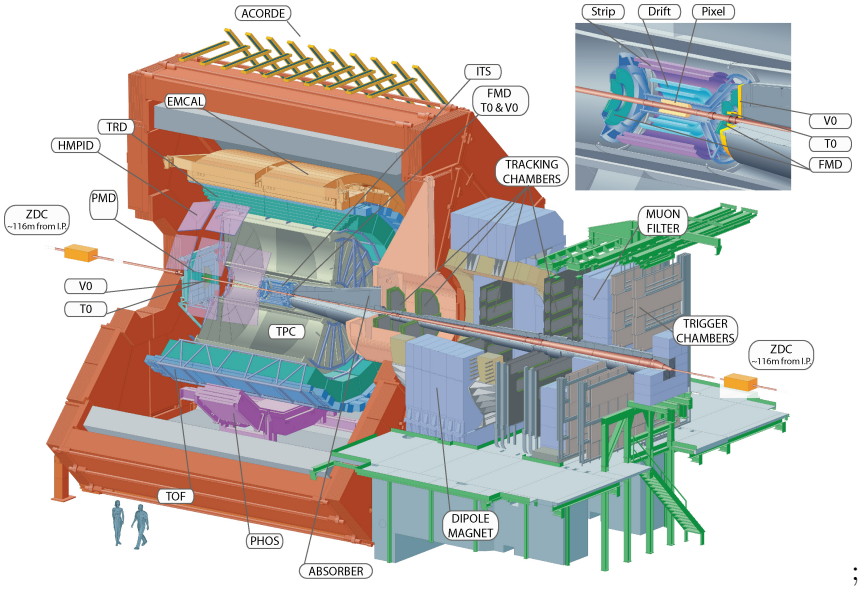


Figure 1. Schematic layout of the ALICE detector with its main subsystems.

identification detectors which exploit transition-radiation (TRD) and time-of-flight (TOF) techniques, respectively. Small-area systems for high-p_{T} particle-identification (HMPID), photon and neutral-meson measurements (PHOS) and jet reconstruction (EMCal) complement the central barrel. Thanks to these unique features the experiment is able to identify hadrons in a wide momentum range by employing different detection systems and techniques, as discussed in Section 2. The detectors which cover larger rapidity regions include a single-arm muon spectrometer covering the pseudorapidity range -4.0 $\leq \eta \leq$ -2.4 and several smaller detectors (VZERO, TZERO, FMD, ZDC, and PMD) for triggering, multiplicity measurements and centrality determination. A detailed description of the ALICE detector layout and of its subsystems can be found in [1].

Since November 2009 when the first collisions at the LHC occurred, the ALICE experiment has collected proton-proton data at several centre-of-mass energies ($\sqrt{s}$ = 0.9, 2.76, 7 and 8 TeV). During the first two LHC heavy-ion runs, in 2010 and 2011, the detector recorded Pb–Pb collisions at a centre-of-mass energy per nucleon pair of $\sqrt{s_{\mathrm{NN}}} = 2.76$ TeV and could profit from of an integrated luminosity of about 10 $\mu\mathrm{b}^{-1}$ and 100 $\mu\mathrm{b}^{-1}$, respectively. It is worth stressing the outstanding performance of the LHC complex: the instant luminosity exceeded $10^{26}\mathrm{cm}^{-2}\mathrm{s}^{-1}$ in the second run, higher than the design value. Proton-lead (p–Pb) collision data were also collected with the ALICE detector. This occurred during a short run performed in September 2012 in preparation for the main p–Pb run at the beginning of 2013. Eight pairs of bunches collided in the ALICE interaction region, providing a luminosity of about $8 \times 10^{25}\mathrm{cm}^{-2}\mathrm{s}^{-1}$. The configuration (4 TeV protons colliding with fully stripped ^{208}Pb ions at 82×4 TeV) resulted in interactions at $\sqrt{s_{\mathrm{NN}}} = 5.02$ TeV in the nucleon-nucleon centre-of-mass system, which moves with a rapidity of $\Delta y_{\mathrm{NN}} = 0.465$.

2. Particle identification

In this section the main particle-identification (PID) detectors relevant to the analyses presented in this paper are briefly discussed. A detailed review of the ALICE experiment and of its PID capabilities can be found in [2]. The ITS is the innermost detector system, a six-layer silicon detector located at radii between 4 and 43 cm. Four of the six layers provide specific energy loss $\mathrm{d}E/\mathrm{d}x$ measurements and are used for particle identification in the non-relativistic $(1/\beta^2)$

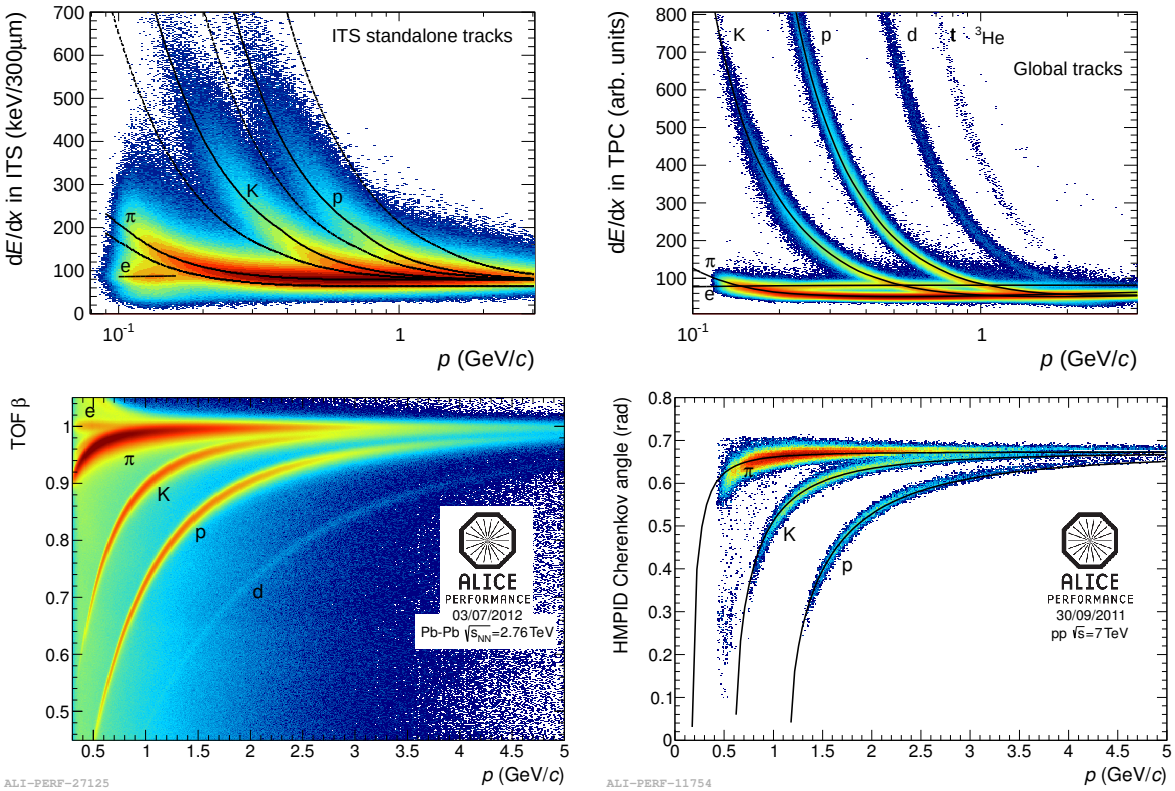


Figure 2. Energy loss $\mathrm{d}E/\mathrm{d}x$ in the ITS (top-left) and in the TPC (top-right). The continuous curves represent the Bethe-Bloch parametrization. (bottom-left) particle velocity β measured with TOF as a function of momentum. (bottom-right) Cherenkov angle measured in the HMPID as a function of the track momentum.

region. By using the ITS as a standalone tracker it is possible to reconstruct and identify low-momentum particles (below 200 MeV/c) not reaching the main tracking systems (Figure 2 top-left). The TPC is the main central-barrel tracking detector of ALICE. It provides three-dimensional hit information and specific energy-loss measurements with up to 159 samples. With the measured particle momentum and $\langle \mathrm{d}E/\mathrm{d}x \rangle$ the particle type can be determined by comparing the measurements with the Bethe-Bloch expectation (Figure 2 top-right). The TOF detector is a large-area array of Multigap Resistive Plate Chambers (MRPC) and covers the central pseudorapidity region ($|\eta| < 0.9$, full azimuth). Particle identification is performed by matching momentum and trajectory-length measurements performed by the tracking system with the time-of-flight information provided by the TOF system. The overall time-of-flight resolution is measured to be about 85 ps in Pb–Pb collisions (about 120 ps in pp collisions) and it is determined by the time resolution of the detector itself and by the start-time resolution (Figure 2 bottom-left). The HMPID detector consists of seven identical proximity focusing RICH (Ring Imaging Cherenkov) counters. Photon detection is performed using the proportional multiwire chambers coupled to pad-segmented CsI photocathode. Particle identification is obtained by means of the measurement of the Cherenkov angle allowing the separation of pions and kaons between 1 GeV/c and 3 GeV/c and protons from 1.5 GeV/c up to 5 GeV/c (Figure 2).

The transverse momentum spectra of primary $\pi^{\pm}$, $\mathrm{K}^{\pm}$, p and $\bar{\mathrm{p}}$ are measured at mid-rapidity ($|y| < 0.5$) combining the techniques and detectors described above. Primary particles are defined as prompt particles produced in the collision and all decay daughters, except products

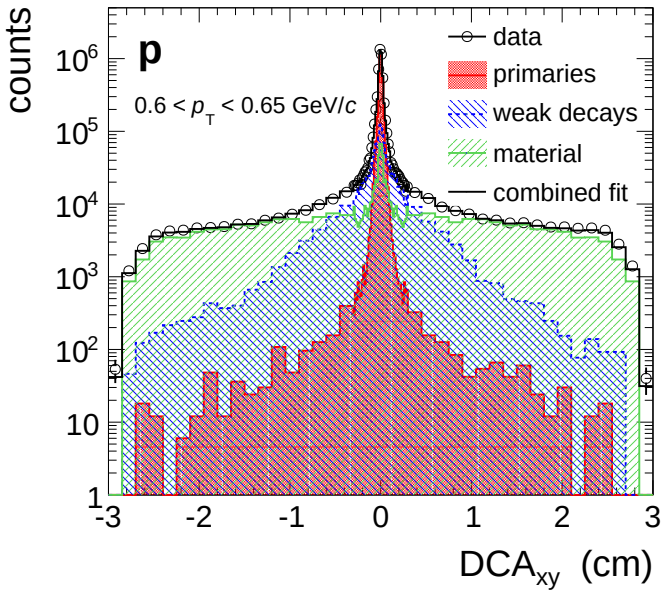


Figure 3. Transverse DCA (DCA_{xy}) of protons in the range between 0.6 GeV/c and 0.65 GeV/c in 0-5% most central Pb–Pb collisions together with the Monte Carlo templates which are fitted to the data.

from weak decays of strange particles. The contribution from the feed-down of weakly-decaying particles to $\pi^{\pm}$, p and $\bar{\text{p}}$ and from protons emitted from secondary interactions with material are subtracted by fitting the data using Monte Carlo templates of the DCA[1] distributions (Figure 3). Particles can also be identified in ALICE via their characteristics decay topology or invariant mass. This, combined with the direct identification of the decay daughters, allows one to reconstruct weakly-decaying particles and hadronic resonances with a good signal-to-background ratio.

3. Light-flavour hadron production

ALICE has measured the production yields of primary charged pions, kaon and (anti)protons in a wide momentum range and in several colliding systems. The measurements have been performed in proton-proton collisions at several centre-of-mass energies ($\sqrt{s}$ = 0.9, 2.76 and 7 TeV) and in Pb–Pb collisions at $\sqrt{s_{\rm NN}}$ = 2.76 TeV as a function of collision centrality.

In Pb–Pb collisions the transverse momentum $p_{\rm T}$ distributions and yields are compared to previous results at RHIC and expectations from hydrodynamic and thermal model. The results obtained for central Pb–Pb collisions are shown in Figure 4 and 5. The spectral shapes are harder than those observed at RHIC, indicating an increase of the radial flow velocity with the centre-of-mass energy. The radial flow at the LHC is found to be about 10% higher than at RHIC energy. The hydrodynamic models shown in Figure 4 give for central collisions a fair description of the data, describing the experimental spectra within 20%. This supports a hydrodynamic interpretation of the transverse momentum distribution in central collisions at the LHC. Further details of this anaysis and the models used to compare with the data can be found in [5].

While the K/π integrated production ratio is observed to be in line with lower energy measurements and predictions from the thermal model, both the p/π and the Λ/π ratios are

[1] Distance of Closest Approach to the reconstructed primary vertex.

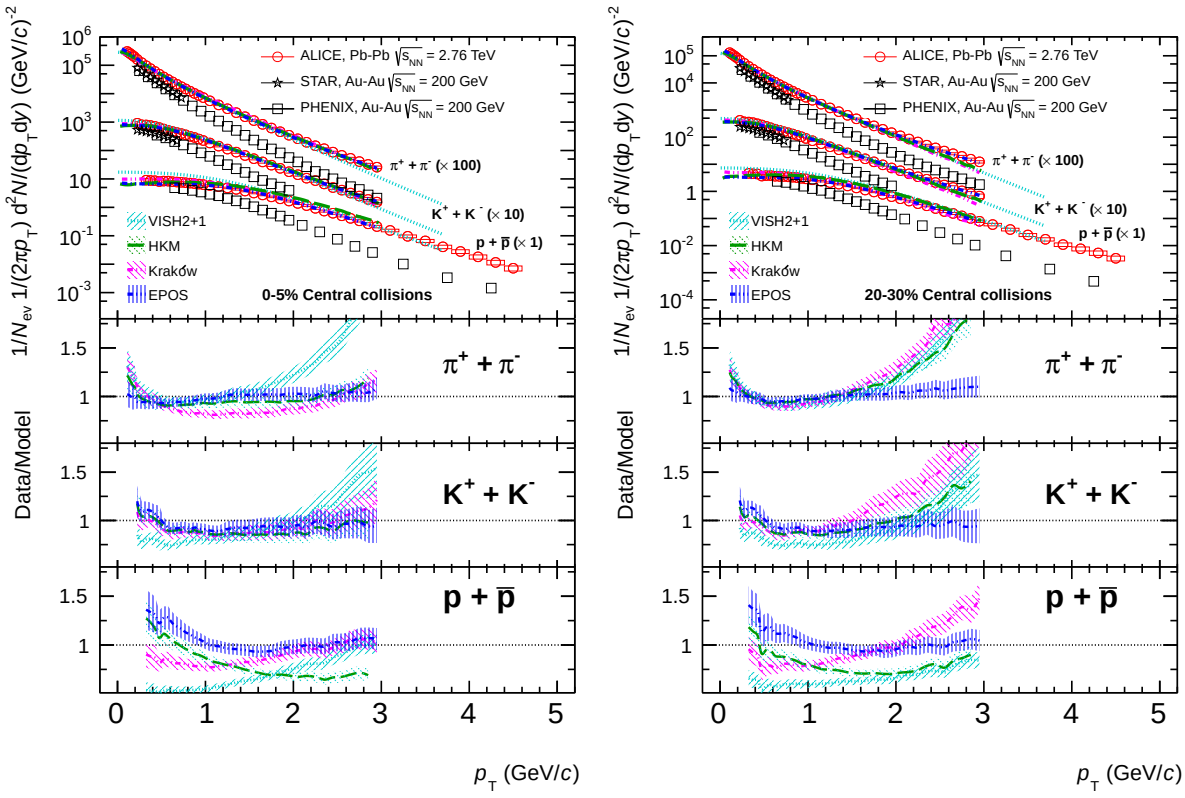


Figure 4. Transverse momentum distributions of the sum of positive and negative pions, kaons and protons for central Pb–Pb collisions. The results are compared to RHIC data and hydrodynamic models.

lower than those at RHIC and significantly lower (a factor $\sim$ 1.5 and 1.35, respectively) than predictions. A possible explanation of these deviations from the thermal-model predictions may be re-interactions in the hadronic phase due to large cross sections for antibaryon-baryon annihilation [6, 7, 8].

The p_{T}-dependent yield of charged kaons and protons normalized to charged pions are shown in Figure 6 for pp collisions at $\sqrt{s} = 2.76$ and 7 TeV where they are compared with theoretical model predictions. Within the experimental uncertainties no energy dependence is observed in the data. The observed production ratios are not reproduced by NLO calculations [9]. PYTHIA Monte Carlo generator [10] underpredicts the proton-to-pion ratio at intermediate p_{T}.

Pion, kaon and (anti)proton production in Pb–Pb collisions have been compared to that in pp collisions and all show a suppression pattern which is similar to that of inclusive charged hadrons at high momenta (p_{T} above $\simeq$ 10 GeV/c), as shown in Figure 7 and 8 [11]. This seems to suggest that the dense medium formed in Pb–Pb collisions does not affect the fragmentation. A similar conclusion can be drawn from the proton-to-pion ratio measured in Pb–Pb collisions (Figure 9 and 10): for intermediate momenta (3–7 GeV/c) it exibits a relatively strong enhancement, by a factor of 3 compared to that in pp collisions at $p_{\mathrm{T}} \approx 3$ GeV/c and returns to the value in pp collisions at higher momenta (p_{T} above $\simeq$ 10 GeV/c) [11]. A similar observation was also reported for the $\Lambda/\mathrm{K}^0_{\mathrm{s}}$ ratio and possible explanations have been proposed which include particle production via quark recombination [12].

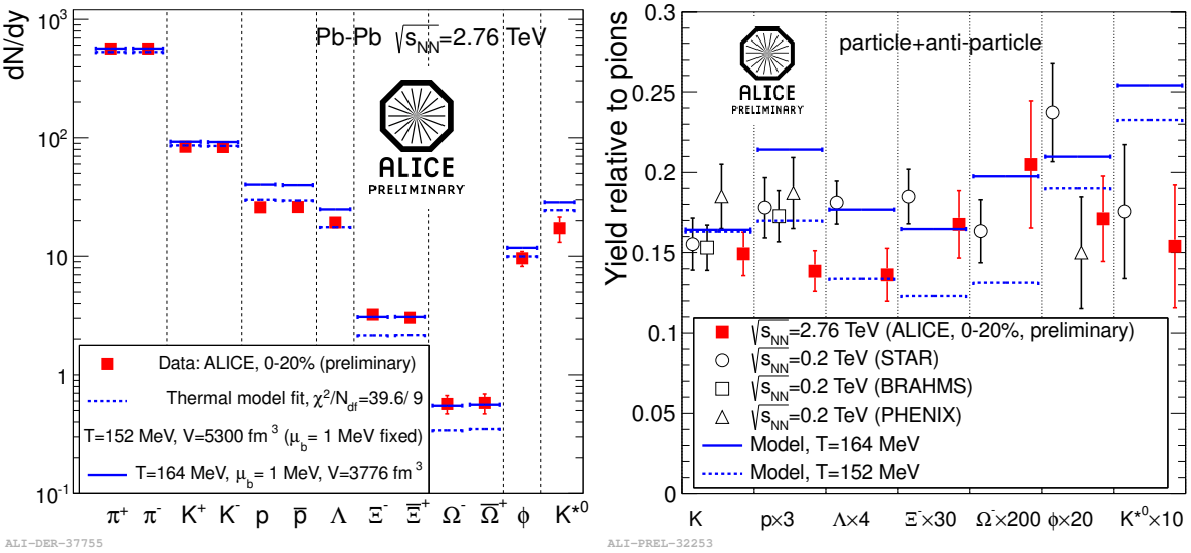


Figure 5. (left) The thermal fit of ALICE data showing data and model for the best fit. (right) Mid-rapidity particle ratios compared to RHIC results and predictions from thermal models for central Pb–Pb collisions at the LHC.

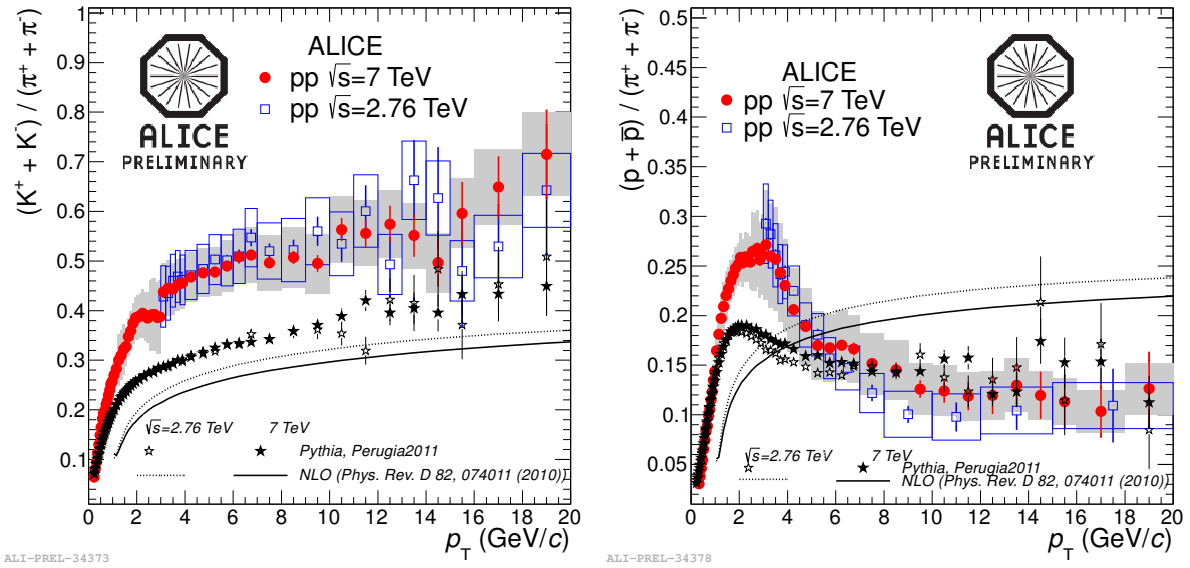


Figure 6. K/π (top) and p/π production ratio in pp collisions compared with PYTHIA Monte Carlo predictions and NLO calculations.

4. Transverse momentum distribution in proton-lead collisions

Particle production in proton-lead (p–Pb) collisions allows one to study and understand QCD at low parton fractional momentum x and high gluon density. It is moreover expected to be sensitive to nuclear effects in the initial state. For this reason p–Pb measurements provide an essential reference tool to discriminate between initial and final state effects and they are crucial for the studies and the understanding of deconfined matter created in nucleus-nucleus collisions.

The measurement of the transverse momentum p_T distributions of charged particle in p–Pb collisions were reported already in [13]. It was previously shown that the production of

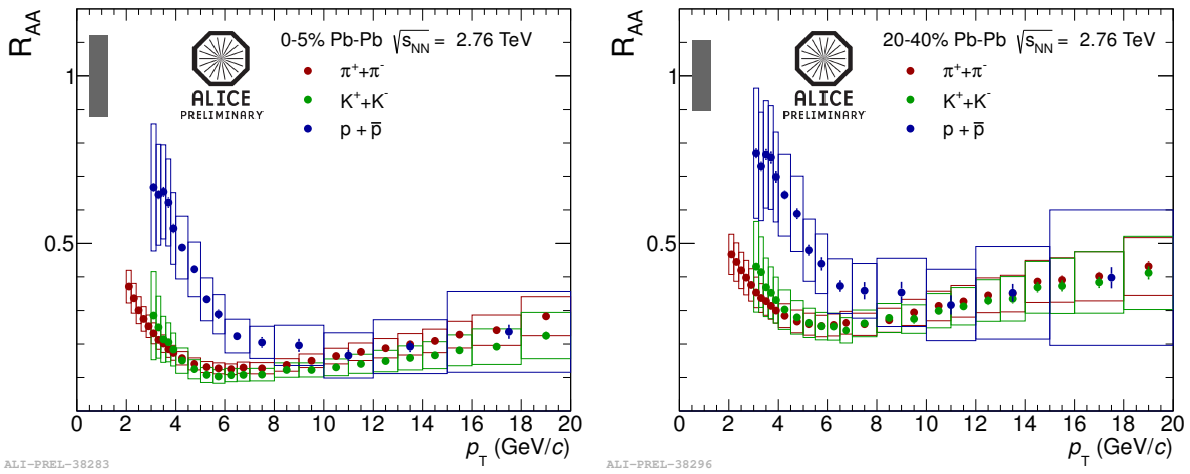


Figure 7. Charged pion, kaon and (anti)proton nuclear modification factor R_{AA} as a function of p_T for Pb–Pb collisions at $\sqrt{s_{NN}} = 2.76$ TeV for centrality 0-5% (left) and 20-40% (right). Statistical (vertical error bars) and systematic (gray and colored boxes) are shown for the charged pion RAA. The gray boxes contains the common systematic error related to pp normalization to INEL and N_{coll}.

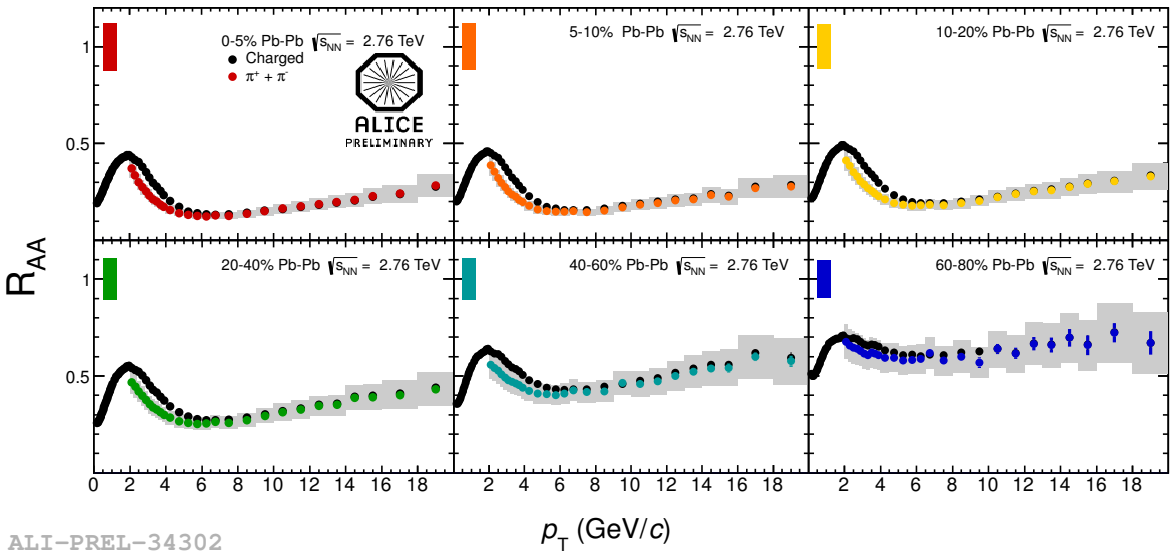


Figure 8. Nuclear modification factor R_{AA} of charged pions compared to the R_{AA} of unidentified charged particles as a function of p_T for different centrality classes. Statistical (vertical error bars) and systematic (gray and colored boxes) errors are shown for the charged pions. The colored boxes contain the common systematic uncertainty related to the number of binary collisions and the pp normalization to INEL. Only statistical errors are shown for the unidentified charged R_{AA}.

charged hadrons in central Pb–Pb collisions at the LHC is strongly suppressed [14, 15]. The suppression remains substantial up to 100 GeV/c and is also seen in reconstructed jets [16]. Proton-lead collisions provide a control experiment to clearly establish whether the initial state of the colliding nuclei plays a role in the observed high-p_T hadron production in Pb–Pb collisions. In

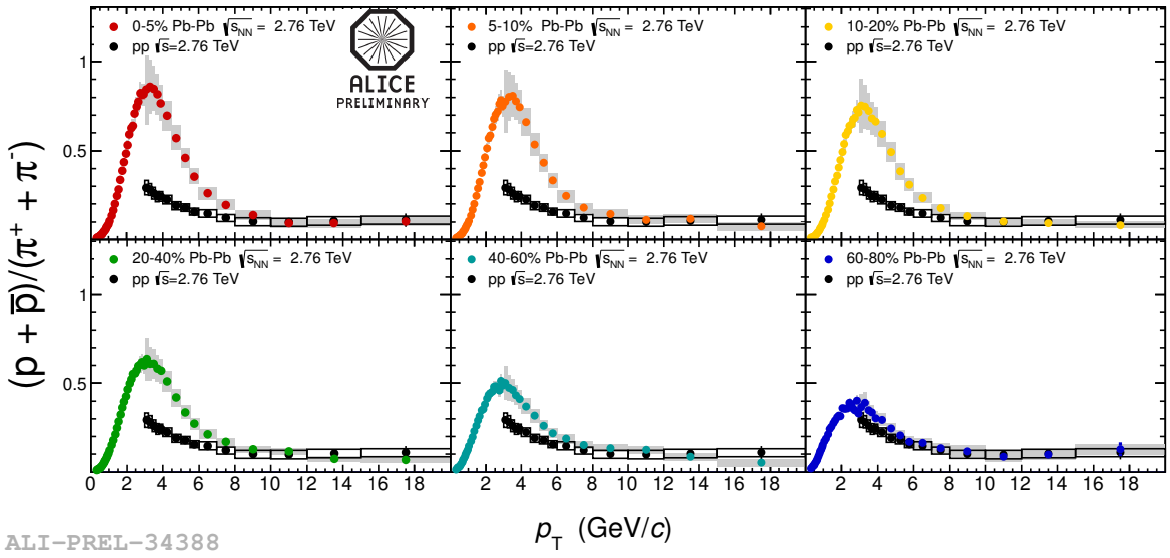


Figure 9. Proton-to-pion ratio in Pb–Pb collisions compared with pp results at 2.76 TeV in several centrality bins. In Pb–Pb the statistical and systematic uncertainties are displayed as error bars and gray bands, respectively. In pp the systematic uncertainty is displayed in black squares.

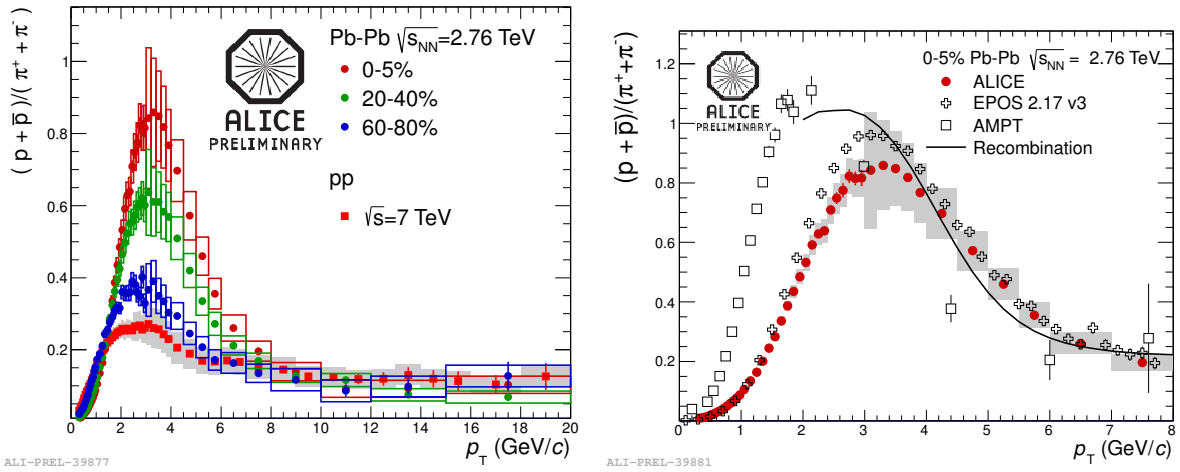


Figure 10. (left) Proton-to-pion ratio in Pb–Pb collisions in several centrality bins compared with pp results at 2.76 TeV. (right) Proton-to-pion ratio in central Pb–Pb collisions compared with models.

order to quantify nuclear effects, the p_{T}-differential yield relative to the proton-proton reference, the so-called nuclear modification factor, is calculated. The nuclear modification factor is expected to be unity for hard processes which exhibit binary collision scaling. This has been recently confirmed in Pb–Pb collisions at the LHC by the measurements of direct photon [17], Z^0 [18] and $\mathrm{W}^{\pm}$ [19], observables which are not affected by hot QCD matter. In Figure 11 the measurement of the nuclear modification factor in p–Pb collisions $\mathrm{R_{pPb}}$ is compared to that in central (0-5% centrality) and peripheral (70–80%) Pb–Pb collisions $\mathrm{R_{PbPb}}$. $\mathrm{R_{pPb}}$ is observed to be consistent with unity for transverse momenta higher than about 2 GeV/c. This important

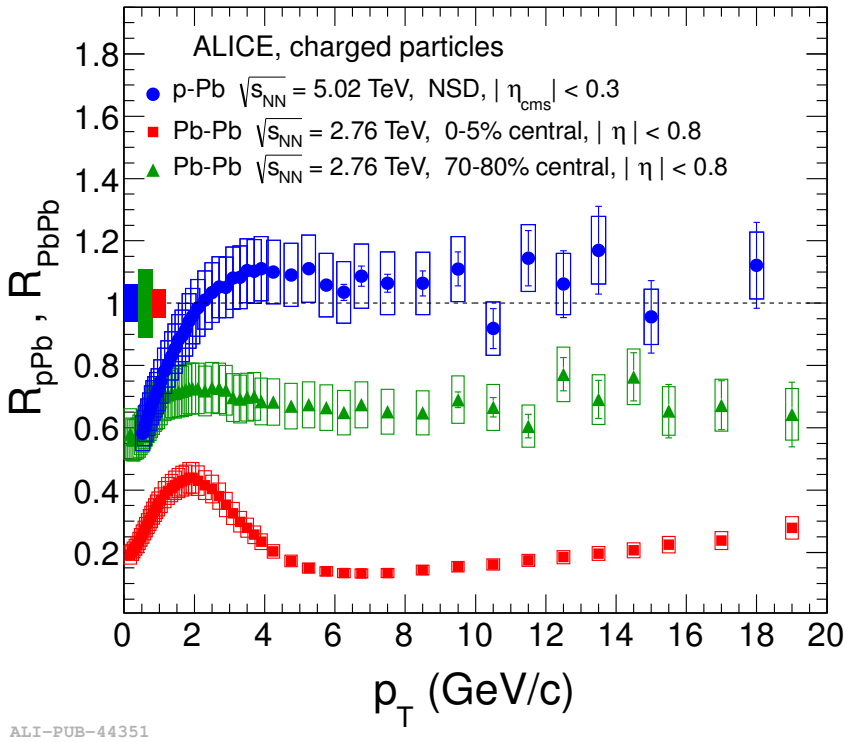


Figure 11. The nuclear modification factor of charged particles as a function of transverse momentum in NSD p–Pb collisions at $\sqrt{s_{\rm NN}} = 5.02$ TeV compared to measurements in central (0-5%) and peripheral (70-80%) Pb–Pb collisions at $\sqrt{s_{\rm NN}} = 2.76$ TeV.

measurement demonstrates that the strong suppression observed in central Pb–Pb collisions at the LHC is not due to an initial-state effect, but it is a final state effect related to the hot matter created in high-energy heavy-ion reactions.

5. Summary and conclusions

ALICE has obtained so far a wealth of physics results both from the analysis of proton-proton collision data and from the first two LHC heavy-ion runs.

The transverse momentum spectra of $\pi^{\pm}$, $K^{\pm}$, p and $\bar{p}$ have been measured with ALICE in several colliding systems and energies at the LHC demonstrating the excellent PID capabilities of the experiment. Data in pp collisions show no evident $\sqrt{s}$ dependence in hadron production ratios. In Pb–Pb collisions $\bar{p}/\pi^-$ integrated ratio is significantly lower than statistical model predictions with a chemical freeze-out temperature $T_{ch} \simeq 160-170$ MeV. The average transverse momenta and the transverse momentum spectra indicate a ∼10% stronger radial flow than at RHIC energies.

In the intermediate transverse momentum $p_{\rm T}$ region, an enhancement of the baryon-to-meson ratio is observed. The maximum of the ratio is shifted to higher $p_{\rm T}$ with respect to RHIC measurements. The results of the measurements of charged pion, kaon, protons and antiproton production at high $p_{\rm T}$ were also presented. The nuclear modification factors for these species are similar in magnitude, suggesting that the medium does not significantly affect fragmentation.

First results from a short pilot run with proton-lead beams have been also reported. The measurement of the charged-particle transverse momentum $p_{\rm T}$ spectra and nuclear modification factor in p–Pb collisions at $\sqrt{s_{\rm NN}} = 5.02$ TeV, covering $0.5 < p_{\rm T} < 20$ GeV/c, show a nuclear

modification factor consistent with unity for $p_{\rm T} > 2$ GeV/c. This measurement indicates that the strong suppression of hadron production at high $p_{\rm T}$ observed at the LHC in Pb–Pb collisions is not due to an initial-state effect, but is the fingerprint of jet quenching in hot QCD matter.

References

[1] K. Aamodt *et al.* [ALICE Collaboration], "The ALICE experiment at the CERN LHC", JINST **3** (2008) S08002.
[2] G. Alessandro, (Ed.) *et al.* [ALICE Collaboration], "ALICE: Physics performance report, volume II", J. Phys. G **32** (2006) 1295.
[3] B. Abelev *et al.* [ALICE Collaboration], "Pseudorapidity density of charged particles p-Pb collisions at $\sqrt{s_{NN}} = 5.02$ TeV", arXiv:1210.3615 [nucl-ex].
[4] B. Alver, M. Baker, C. Loizides and P. Steinberg, "The PHOBOS Glauber Monte Carlo", arXiv:0805.4411 [nucl-ex].
[5] B. Abelev *et al.* [ALICE Collaboration], "Pion, Kaon, and Proton Production in Central Pb–Pb Collisions at $\sqrt{s_{NN}} = 2.76$ TeV", Phys. Rev. Lett. **109** (2012) 252301 [arXiv:1208.1974 [hep-ex]].
[6] J. Steinheimer, J. Aichelin and M. Bleicher, "Non-thermal p/π ratio at LHC as a consequence of hadronic final state interactions", arXiv:1203.5302 [nucl-th].
[7] F. Becattini, M. Bleicher, T. Kollegger, M. Mitrovski, T. Schuster and R. Stock, "Hadronization and Hadronic Freeze-Out in Relativistic Nuclear Collisions", Phys. Rev. C **85** (2012) 044921 [arXiv:1201.6349 [nucl-th]].
[8] Y. Pan and S. Pratt, "Baryon Annihilation in Heavy Ion Collisions", arXiv:1210.1577 [nucl-th].
[9] R. Sassot, P. Zurita and M. Stratmann, "Inclusive Hadron Production in the CERN-LHC Era", Phys. Rev. D **82** (2010) 074011 [arXiv:1008.0540 [hep-ph]].
[10] P. Z. Skands, Phys. Rev. D **82** (2010) 074018 [arXiv:1005.3457 [hep-ph]].
[11] A. Ortiz Velasquez [ALICE Collaboration], "Production of pions, kaons and protons at high p_T in $\sqrt{s_{NN}} =$ 2.76 TeV Pb-Pb collisions", arXiv:1210.6995 [hep-ex].
[12] R. J. Fries, B. Muller, C. Nonaka and S. A. Bass, "Hadronization in heavy ion collisions: Recombination and fragmentation of partons", Phys. Rev. Lett. **90** (2003) 202303 [nucl-th/0301087].
[13] B. Abelev *et al.* [ALICE Collaboration], "Transverse Momentum Distribution and Nuclear Modification Factor of Charged Particles in p-Pb Collisions at $\sqrt{s_{NN}} = 5.02$ TeV", arXiv:1210.4520 [nucl-ex].
[14] K. Aamodt *et al.* [ALICE Collaboration], "Suppression of Charged Particle Production at Large Transverse Momentum in Central Pb–Pb Collisions at $\sqrt{s_{NN}} = 2.76$ TeV", Phys. Lett. B **696** (2011) 30 [arXiv:1012.1004 [nucl-ex]].
[15] B. Abelev *et al.* [ALICE Collaboration], "Centrality Dependence of Charged Particle Production at Large Transverse Momentum in Pb–Pb Collisions at $\sqrt{s_{\rm NN}} = 2.76$ TeV", [arXiv:1208.2711 [hep-ex]].
[16] G. Aad *et al.* [ATLAS Collaboration], "Measurement of the jet radius and transverse momentum dependence of inclusive jet suppression in lead-lead collisions at $\sqrt{s_{NN}} = 2.76$ TeV with the ATLAS detector", arXiv:1208.1967 [hep-ex].
[17] S. Chatrchyan *et al.* [CMS Collaboration], "Measurement of isolated photon production in pp and PbPb collisions at $\sqrt{s_{NN}} = 2.76$ TeV", Phys. Lett. B **710** (2012) 256 [arXiv:1201.3093 [nucl-ex]].
[18] S. Chatrchyan *et al.* [CMS Collaboration], "Study of Z boson production in PbPb collisions at nucleon-nucleon centre of mass energy = 2.76 TeV", Phys. Rev. Lett. **106** (2011) 212301 [arXiv:1102.5435 [nucl-ex]].
[19] S. Chatrchyan *et al.* [CMS Collaboration], "Study of W boson production in PbPb and pp collisions at $\sqrt{s_{NN}} = 2.76$ TeV", Phys. Lett. B **715** (2012) 66 [arXiv:1205.6334 [nucl-ex]].